

Collision-induced absorption in the ν_2 fundamental band of CH₄. I. Determination of the quadrupole transition moment

R. H. Tipping and Alex Brown

Department of Physics and Astronomy, University of Alabama, Tuscaloosa, Alabama 35487

Q. Ma

Department of Applied Physics, Columbia University, and Institute for Space Studies, Goddard Space Flight Center, New York, New York 10025

J. M. Hartmann and C. Boulet

Laboratoire de Photophysique Moléculaire, CNRS, Bât. 350, Université Paris-Sud, Campus d'Orsay, Orsay 91405 Cedex, France

J. Liévin

Laboratoire de Chimie Physique Moléculaire, CP 160/09, Université Libre de Bruxelles, Ave. F. D. Roosevelt, 50, B-1050, Bruxelles, Belgium

(Received 11 July 2001; accepted 15 August 2001)

An experimental value for the quadrupole transition moment of the ν_2 fundamental band of CH₄ has been determined by fitting the collision-induced enhancement spectrum of CH₄ with Ar as the perturber. The observed quadrupole-induced absorption increases linearly with the Ar density, ρ_{Ar} , and is comparable to the allowed dipole intensity due to Coriolis interaction with the ν_4 band at approximately 125 amagats. Ignoring vibration-rotation interaction and Coriolis interaction, we equate the measured slope of the integrated intensity versus ρ_{Ar} to the theoretical expression for the quadrupole-induced absorption, and obtain the value $|\langle 0|Q|\nu_2\rangle|=0.445 ea_0^2$ for the quadrupole transition matrix element. A theoretical value $\langle 0|Q|\nu_2\rangle=0.478 ea_0^2$ has been determined by large-scale *ab initio* calculations and, considering both the theoretical approximations and experimental uncertainties, we regard the agreement as good, thus confirming our interpretation of the enhancement as due to the quadrupole collision-induced mechanism. © 2001 American Institute of Physics. [DOI: 10.1063/1.1408915]

I. INTRODUCTION

The infrared absorption by CH₄ is important in many applications, from combustion studies to planetary atmospheres. As a consequence, there exists in the literature a large number of papers on the various infrared (IR) and Raman bands of pure methane and methane-perturber mixtures.¹ Many of these works were carried out at low densities, but there also exist a number of studies of allowed and collision-induced absorption (CIA), mainly in the translation-rotation region,^{2,3} carried out using large perturber pressures.

More recently, in a series of four papers,⁴⁻⁷ Pieroni *et al.* have carried out systematic studies of a number of Raman and IR transitions using both rare gases and N₂ as perturbers over a large range of densities and temperatures in order to investigate the role of line mixing.⁸ Using a model for the construction of the relaxation matrix starting from state-to-state rates calculated by a semiclassical approach, they were able to obtain good agreement between theory and experiment for the ν_3 fundamental and the Raman Q branch of the ν_1 band. In the most recent paper of the series,⁷ they presented new experimental spectra in the ν_4 and ν_2 spectral region (1200–2000 cm⁻¹) and compared these results with their line-mixing model without introducing any additional parameters. For the ν_4 region, very good agreement was obtained for CH₄-N₂ mixtures up to 300 amagat of N₂. In the

ν_2 region, satisfactory agreement was obtained for small N₂ densities, but as the density was increased, they observed the appearance of a broad additional absorption beneath the allowed ν_2 lines; this enhancement increased linearly with perturber density and was comparable to the Coriolis-allowed intensity at approximately 125 amagat. No similar changes with He as the perturber was seen even at higher densities.⁷

The physical origin of the enhancement was unclear, but three possible mechanisms were proposed:⁷ the far wings of the stronger ν_4 band, the formation of CH₄-X complexes (X=He, Ar, or N₂), and collision-induced absorption.⁹ The first mechanism was considered unlikely because of the good agreement in the high-frequency wing of the ν_4 band.⁷ The second possible mechanism is consistent with the absence of the enhancement with He, because the potential well in this case is very shallow. Furthermore, if the anisotropic interaction were small so that the molecules could rotate freely in the complex, the resulting dimer spectrum would appear in the same spectral region; except for bound-bound transitions (expected to be weak at room temperature), the dimer transitions would be broad and the resulting absorption would be similar to the CIA resulting from free-free transitions in a colliding pair. With N₂ as the perturber, there would be CIA from the induced dipole moment arising from the quadrupole moment of N₂ and the anisotropic polarizability of CH₄; this could appear in the ν_2 region because this fundamental is

Raman active. However, this mechanism would not be present if the perturber were a rare gas. This is consistent with the observations with He, but inconsistent with previous¹⁰ and the present more accurate results with Ar. In fact, both Ar and N₂ have comparable enhancements and other, more polarizable gases have larger enhancements.¹¹

Another possible CIA mechanism is due to the dipole-induced dipole, where the (small Coriolis-allowed) dipole of methane would interact with both the isotropic polarizability (α) of Ar or N₂ producing "single transitions" or with the anisotropic polarizability (γ) of N₂ producing "double transitions." However, a calculation of this latter effect results in an absorption that is too weak to explain the observed results.

In the present article, we propose another collision-induced dipole mechanism, namely, the vibrating quadrupole of CH₄ interacting with the polarizability of the perturber. This mechanism would be present for absorption in the ν_2 region, even in the absence of Coriolis interaction, because this band is also quadrupole-allowed; that is, there is a non-vanishing quadrupole transition matrix element between the ground and ν_2 vibrational states. This mechanism is consistent with the fact that CH₄-Ar and CH₄-N₂ have comparable enhancements since both perturbers have comparable values of α , whereas the absorption would be much smaller for CH₄-He due to its smaller polarizability.

In the present article, we will concentrate on the simplest case of CH₄-Ar. By equating the slope of the experimentally determined integrated intensity in the spectral range 1410–2000 cm⁻¹ versus the density ρ_{Ar} to the theoretical result, calculated assuming no vibration-rotation interaction or Coriolis interaction, we can obtain a value for the magnitude of the $\langle 0|Q|\nu_2\rangle$ transition moment, which is the only unknown quantity. This transition moment would be very difficult to obtain experimentally, for example, from intensity measurements of the allowed quadrupole spectrum because of the weakness of the quadrupole transitions and the complications arising from the Coriolis interaction. To the best of our knowledge, no *ab initio* value of $\langle 0|Q|\nu_2\rangle$ has been published heretofore, so we have carried out extensive calculations for comparison with the experimental results.

II. EXPERIMENTAL DETAILS

The measurements have been made with the experimental apparatus and procedures described in Refs. 4–7. A 21 cm long cell capable of withstanding pressures up to 400 atm is used together with a Fourier transform spectrometer. For the Ar measurements, mixtures of approximately 1.5 atm of CH₄ with 380 atm of Ar have been used. Spectra are then recorded starting from this sample and then lowering the total pressure of the mixture. The recordings cover the 1000–6500 cm⁻¹ spectral range, thus they extend over the ν_2 band, but also include transitions belonging to the $\nu_3 + \nu_4$ (4000–4700 cm⁻¹) and $2\nu_3$ (5500–6200 cm⁻¹) bands. The latter are used for a check of the amounts of CH₄ in the mixture from a determination of the associated integrated intensities using the HITRAN database.¹² Typical spectra for various densities in the ν_2 spectral region are plotted in Fig. 1. They show a behavior similar to that observed for

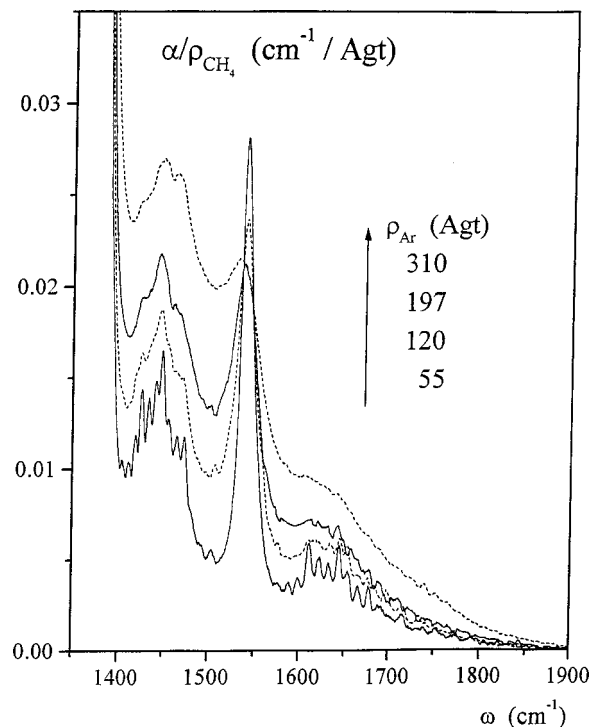


FIG. 1. Typical results for $\alpha(\omega)/\rho_{\text{CH}_4}$ in cm⁻¹/agt vs ω in cm⁻¹ for increasing values of ρ_{Ar} in the ν_2 spectral region.

CH₄-N₂ spectra;⁷ i.e., the growth of a background absorption below the Coriolis-allowed ν_2 absorption with increasing perturber density. The integrated absorption coefficient between 1410 and 2000 cm⁻¹ divided by ρ_{CH_4} is plotted versus ρ_{Ar} and the results are shown in Fig. 2. The results are similar to those obtained for CH₄-N₂ mixtures.⁷ We note that the intercept is in good agreement with that obtained for the allowed transition in this region calculated using the HITRAN data.

III. THEORY

A. Collision-induced absorption

In this section, we will review briefly the theoretical calculation of the integrated intensity of the CIA ν_2 band for

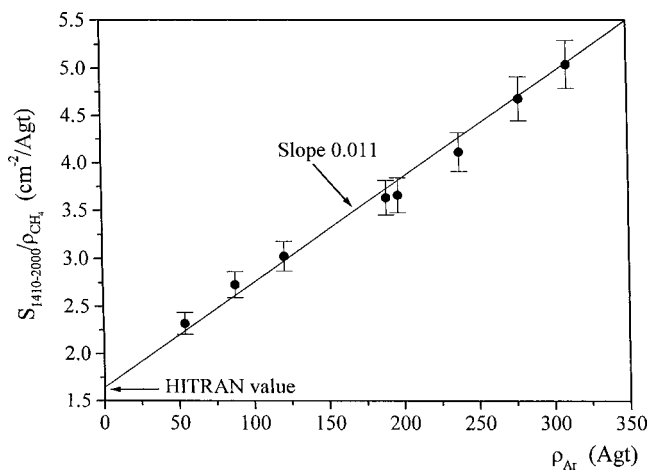


FIG. 2. The integrated absorption coefficient between 1410 and 2000 cm⁻¹ divided by ρ_{CH_4} in cm⁻²/agt plotted vs ρ_{Ar} .

CH₄-Ar mixtures. From the work of Poll and co-workers,^{13,14} one can obtain the following expression for the slope of the integrated intensity versus the density of Ar in units of cm⁻²/agt²:

$$\begin{aligned} 1/\rho_{\text{Ar}}\rho_{\text{CH}_4} \int \alpha(\omega) d\omega &= (4\pi^2/3)\alpha_F n_0^2 a_0^5 \sum_{c,J,J'} \omega_{0J,\nu_2 J'} \\ &\times P_J C(J\lambda J';00)^2 \langle B_C(R)^2 \rangle. \end{aligned} \quad (1)$$

In this expression, ρ_{Ar} and ρ_{CH_4} are the densities in amagat, $\alpha(\omega)$ is the absorption coefficient in cm⁻¹ at frequency ω (cm⁻¹) and the integral is taken over the extent of the ν_2 band from approximately 1410 to 2000 cm⁻¹, α_F is the fine structure constant, n_0 is the number density at standard temperature and pressure, a_0 is the Bohr radius, $\omega_{0J,\nu_2 J'}$ are the methane vibration-rotation frequencies, and $C(J\lambda J';00)$ is a Clebsch-Gordan coefficient. As in previous studies on methane,¹⁴ we ignore the slight dependence on the other rotational quantum numbers. In general, the index c represents the set of numbers needed to specify the induced-dipole moment components, but in the present case we consider only one mechanism: the isotropic quadrupole induction having $\lambda=2$, although there are two components corresponding to the doubly degenerate ν_2 state. The function $B(R)$ is the matrix element of this component which is given by¹⁵

$$B(R) = \sqrt{3} \alpha_{\text{Ar}} \langle 0J|Q|\nu_2 J' \rangle / R^4, \quad (2)$$

where α_{Ar} is the polarizability of Ar, $\langle 0J|Q|\nu_2 J' \rangle$ is the quadrupole moment matrix element of CH₄, and R is the distance between the argon atom and the center of mass of CH₄, all in atomic units. The angular brackets indicate the dimensionless average

$$\begin{aligned} \langle B(R)^2 \rangle &= 4\pi \int_0^\infty g(r) B(r)^2 R^2 dr \\ &= 3\alpha_{\text{Ar}}^2 \langle 0J|Q|\nu_2 J' \rangle^2 I(6). \end{aligned} \quad (3)$$

$I(6)$ is a dimensionless integral that can be written in terms of $x \equiv R/a_0$ as

$$I(6) = 4\pi \int_0^\infty \exp(-V_{\text{iso}}(x)/kT) x^{-6} dx, \quad (4)$$

in which we have approximated the pair distribution function, $g(R)$, by the classical limit, $\exp(-V_{\text{iso}}(x)/kT)$, where $V_{\text{iso}}(x)$ is the isotropic interaction potential between Ar and CH₄. The P_J are the normalized Boltzmann factors

$$P_J = \frac{g_J \exp(-E_{\text{rot}}/kT)}{\sum_J g_J \exp(-E_{\text{rot}}/kT)}, \quad (5)$$

where the statistical weights g_J are taken from Herzberg.¹⁶ Both the rotational energy levels in the ground state and the quadrupole transition frequencies, $\omega_{0J,\nu_2 J'}$, are calculated using the rotational constants, $B_0 = 5.24$ cm⁻¹ and $B_{\nu_2} \cong 5.24$ cm⁻¹, and the ν_2 band-center frequency, $\omega_{00} = 1533.3$ cm⁻¹.

Using Eqs. (3) and (4) in Eq. (1), we can write

$$\begin{aligned} 1/\rho_{\text{Ar}}\rho_{\text{CH}_4} \int \alpha(\omega) d\omega &= 4\pi^2 \alpha_F n_0^2 a_0^5 \alpha_{\text{Ar}}^2 I(6) \sum_{J,J'} \omega_{0J,\nu_2 J'} P_J C(J2J';00)^2 \\ &\times \langle 0J|Q|\nu_2 J' \rangle^2. \end{aligned} \quad (6)$$

The integral $I(6)$ was calculated using $V_{\text{iso}}(x)$ from experimental differential cross-section measurements;¹⁷ the value we obtained is 3.38×10^{-4} . If we ignore the small J dependence of the quadrupole transition moment, we can carry out the summations over J and J' ($=J-2$, J , and $J+2$ for the O , Q , and S branches, respectively) and we obtain

$$\begin{aligned} 1/\rho_{\text{Ar}}\rho_{\text{CH}_4} \int \alpha(\omega) d\omega &= 5.55 \times 10^{-2} \\ &\times \langle 0|Q|\nu_2 \rangle^2 \text{ cm}^{-2}/\text{agt}^2. \end{aligned} \quad (7)$$

Equating this to the experimental slope (0.011 ± 0.001) cm⁻²/agt² from Fig. 2, we obtain for the absolute magnitude of the quadrupole transition moment the value $|\langle 0|Q|\nu_2 \rangle| = 0.445 e a_0^2$. We note that because a small fraction of the allowed intensity of the ν_2 band lies outside of the range of integration (mostly under the strong ν_4 band), one would expect some of the collision-induced absorption also to occur outside the range. Therefore, one should regard the experimental value $0.445 e a_0^2$ as a lower limit.

B. *Ab initio* calculations

The traceless electric quadrupole moment tensor Q of a molecule with a clamped nuclear geometry can be written in atomic units as¹⁸

$$\begin{aligned} Q &= \frac{1}{2} \sum_a^N Z_a (3\bar{r}_a \bar{r}_a - \bar{r}_a^2 I) \\ &- \frac{1}{2} \sum_i^n \langle \psi_0 | \sum_i^n (3\bar{r}_i \bar{r}_i - \bar{r}_i^2 I) | \psi_0 \rangle, \end{aligned} \quad (8)$$

where \bar{r}_a and \bar{r}_i refer to vector positions of nuclei and electrons, respectively, Z_a is the atomic number of nucleus a , and I is the unit tensor. The two terms in (8) correspond to the contributions of the N nuclei and n electrons, respectively, and the latter contribution is averaged over the Born-Oppenheimer ground state electronic wave function ψ_0 . The tensor Q depends explicitly on the internal degrees of freedom of the nuclei $\{q_1, q_2, \dots, q_{3N-6}\}$ and thus defines a hypersurface in this $3N-6$ vector space. The vibrational matrix elements are defined by

$$Q_{v,v''} = \langle v'' | Q(q_1, q_2, \dots, q_{3N-6}) | v' \rangle, \quad (9)$$

where the diagonal elements are the expectation values of the quadrupole in a given vibrational state, and the off-diagonal elements are the transition moments. The calculation of (9) is usually carried out¹⁹ by expanding Q around the equilibrium geometry in a Taylor series in terms of the vibrational coordinates q_k :

TABLE I. Equilibrium geometry of methane (in Å) and normalized normal Cartesian displacements q_{2a} and q_{2b} (in $u^{1/2}$ Å) in the body-fixed axis system (from CMRCI/aug-cc-pVTZ calculations).

Atoms	Equilibrium geometry			q_{2a}			q_{2b}		
	X	Y	Z	X	Y	Z	X	Y	Z
C	0	0	0	0	0	0	0	0	0
H	0.629 46	0.629 46	0.629 46	-0.2034	-0.2034	0.4068	0.3523	-0.3523	0
H	-0.629 46	-0.629 46	0.629 46	0.2034	0.2034	0.4068	-0.3523	0.3523	0
H	0.629 46	-0.629 46	-0.629 46	-0.2034	0.2034	-0.4068	0.3523	0.3523	0
H	-0.629 46	0.629 46	-0.629 46	0.2034	-0.2034	-0.4068	-0.3523	-0.3523	0

$$Q = Q^{(0)} + \sum_{k=1}^{3N-6} Q^{(1)} q_k + \sum_{k=1}^{3N-6} \sum_{k'=1}^{3N-6} Q^{(k,k')} q_k q_{k'} + \dots, \quad (10)$$

where $Q^{(0)}$ is the value of the quadrupole at equilibrium and the quantities $Q^{(k)}, Q^{(k,k')}, \dots$ are the successive derivatives with respect to $q_k, q_{k'}, \dots$ calculated at equilibrium. Note that expansion (10) applies to each component $Q_{\alpha\beta}$ ($\alpha, \beta = X, Y$ or Z) of the quadrupole tensor.

We have calculated, using large-scale *ab initio* methods, the transition moments (9) of methane corresponding to the transition from the ground to the ν_2 vibrational mode. Two matrix elements have been calculated

$$\Theta^{(a)} = \langle 0 | Q | \nu_{2a} \rangle \quad (11a)$$

and

$$\Theta^{(b)} = \langle 0 | Q | \nu_{2b} \rangle, \quad (11b)$$

where the indices a and b refer to the twofold degeneracy of the ν_2 mode which transforms as the E symmetry species of point group T_d .

The double harmonic approximation (mechanical and electrical) has been assumed in the calculations; this means that the vibrational wave functions in (9) are approximated by uncoupled harmonic oscillators and that the series in (10) is truncated after the linear terms. The transition moments (11a) and (11b) thus reduce to the following one-dimensional expression in the mass-weighted normal coordinate q_{2p} :

$$\langle 0 | Q | \nu_{2p} \rangle = Q^{(2p)} \langle 0 | q_{2p} | \nu_{2p} \rangle = (h/8\pi^2 c \omega_2) I^{1/2} Q^{(2p)}, \quad (12)$$

where q_{2p} denotes the normal coordinates q_{2a} or q_{2b} , and ω_2 is the harmonic frequency of the ν_2 mode. The nonvanishing rule applied to T_d predicts that matrix elements (11) are nonzero only for the E symmetry components of the quadrupole, namely

$$(2Q_{ZZ} - Q_{XX} - Q_{YY}) \quad \text{and} \quad (Q_{XX} - Q_{YY}). \quad (13)$$

A high level of *ab initio* theory has been adopted in the calculations in order to describe accurately the changes in the charge distribution occurring with the vibrational motion. All calculations were performed with the program MOLPRO²⁰ using the internally contracted multireference configuration interaction method (CMRCI)²¹ and the aug-cc-pVTZ basis set.²² In this approach, all valence orbitals are first optimized by a CASSCF calculation.²³ All single and double excitations with respect to the multireference CASSCF wave function are then included in a second step in a large-scale con-

figuration interaction calculation. All valence electrons are therefore fully correlated. The sizes of the CI matrices are typically of 210 000 configuration state functions (D_2 symmetry). The one-electron basis set is of valence triple-zeta quality, is correlation consistent, includes polarization functions (3*d*, 2*f*, and 3*p*, 2*d* on C and H atoms, respectively), and is augmented by diffuse functions (1*s*, 1*p*, and 1*s* on the C and H atoms, respectively).

The geometry has been first optimized using the quadratic steepest descent following algorithm.²⁴ The harmonic frequencies and the corresponding normal modes coordinates were then obtained from the Hessian matrix, calculated numerically at the previously derived equilibrium geometry. The calculated harmonic frequencies are 3021.5, 1576.5, 3139.3, and 1354.1 cm^{-1} to be compared to the corresponding values derived from experiment:²⁵ 3025.5, 1582.7, 3156.8, and 1367.4 cm^{-1} . The quadrupole tensor (8) has then been calculated as a function of q_{2a} and q_{2b} , over a range corresponding to $\pm 0.02 u^{1/2} a_0$ around the equilibrium geometry.

Because the quadrupole is the first nonzero electric moment induced by the vibrational transition from $\nu_2=0$ to $\nu_2=1$, it follows that its value is independent of the location of the origin of the coordinate system, and that the signs of the different components can be unambiguously determined from quantum mechanical calculations.^{18,26} For that purpose, one must specify the orientation and direction of the body-fixed coordinate system and of the normal Cartesian displacements q_{2a} and q_{2b} . These data are given in Table I. The body-fixed system obeys the general prescription²⁶ for tetrahedral symmetry, namely that the X , Y , and Z axes are parallel to the edges of a cube containing hydrogen nuclei at alternate vertices, with a hydrogen atom occupying the vertex in the positive octant. The mass-weighted normal coordinates are normalized and are given in units $u^{1/2}$ Å. The corresponding displacement vectors can be visualized as shown in Fig. 3. They essentially correspond to HCH bending motions that break the T_d symmetry into a D_2 point-group symmetry, in which the three C_2 rotation axes are colinear to the Cartesian axes system. The vibrational motion obeys the branching rule $E(T_d) \rightarrow 2A(D_2)$.

The calculated variations of Q with respect to both normal coordinate motions are shown in Fig. 3. Given the axial symmetry, the quadrupole tensor is diagonal in the molecular axes. One sees that, for both coordinates, the linear term in (10) is valid, at least in the limit of the small amplitude vibrations considered here. The numerical values of the first

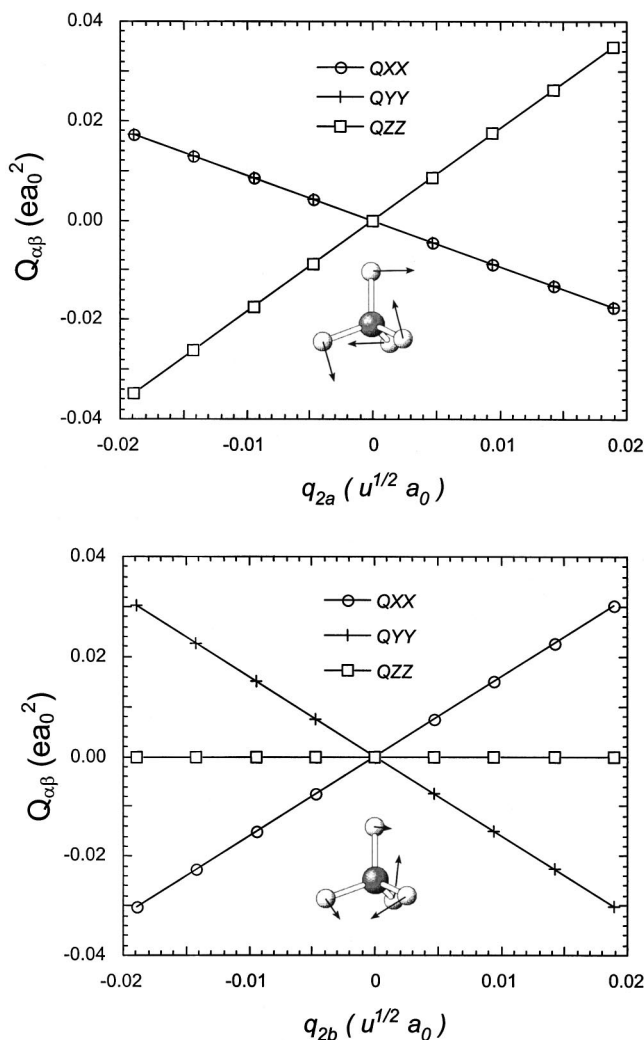


FIG. 3. Variation of the components $Q_{\alpha\beta}$ of the electric quadrupole tensor, Eq. (8), of methane as a function of the normalized mass-weighted normal coordinates q_{2a} and q_{2b} from the CMRCI/aug-cc-pVTZ calculations.

derivatives $Q^{(2a)}$ and $Q^{(2b)}$ and the corresponding quadrupole transition moments (12) are given in Table II.

One can easily verify that the quadrupole induced by the E vibrational mode obeys the symmetry requirement (13) and can be described by a single independent scalar quantity Θ :

$$\Theta = \Theta_{ZZ}^{(a)} = -2\Theta_{XX}^{(a)} = -2\Theta_{YY}^{(a)} \quad (14a)$$

and

TABLE II. First derivatives $Q^{(2a)}$ and $Q^{(2b)}$ of the quadrupole tensor with respect to q_{2a} and q_{2b} (in $e a_0 u^{-1/2}$) and quadrupole tensor transition moment (in $e a_0^2$), induced by the vibrational transition from $\nu_2=0$ to 1 (from CMRCI/aug-cc-pVTZ calculations).

	XX	YY	ZZ
$Q^{(2a)}$	-0.9206	-0.9206	1.8412
$Q^{(2b)}$	1.5946	-1.5946	0
$\langle 0 Q \nu_{2a}\rangle$	-0.1805	-0.1805	$\Theta=0.3610$
$\langle 0 Q \nu_{2b}\rangle$	0.3126	-0.3126	0

$$\Theta_{ZZ}^{(b)} = 0 \quad \text{and} \quad \Theta_{XX}^{(b)} = -\Theta_{YY}^{(b)} = \sqrt{3}/2\Theta. \quad (14b)$$

The contributions of the nuclei and electrons to the total value of $\Theta_{ZZ}^{(a)}$ in Eq. (14a) are calculated to be 0.4477 and $-0.0867 e a_0^2$, respectively. As expected, the contributions have opposite signs and the electronic term accounts for approximately 24% of the final value.

As a test, we have also calculated the quadrupole transition moment at the Hartree-Fock/cc-pVTZ level of approximation; this is a lower level of theory corresponding to significantly less computational costs. The value obtained, $\Theta=0.378 e a_0^2$, is unexpectedly close to the CMCI value.

Because the contributions from the two degenerate vibrational states add incoherently, the theoretical values for the transition moment is

$$|\langle 0|Q|\nu_2\rangle|_{\text{th}} = [\Theta^2 + 3\Theta^2/4]^{1/2} = 0.478 e a_0^2.$$

IV. DISCUSSION AND CONCLUSIONS

The experimental value of the quadrupole matrix element obtained by fitting the $\text{CH}_4\text{-Ar}$ data ($0.445 e a_0^2$) is in good agreement with our *ab initio* calculations ($0.478 e a_0^2$), when one considers both the theoretical approximations and the experimental uncertainty. This leads us to the conclusion that the observed enhancement absorption indeed arises from the quadrupolar induction mechanism considered in the present work. As mentioned previously, the other possible CIA mechanism for $\text{CH}_4\text{-Ar}$ resulting in absorption in the ν_2 region is that due to the Coriolis-allowed dipole-induced dipole, and an estimation of the slope from this mechanism (3×10^{-5}) is far too weak to account for the observations.

The theory presented above is easily generalized in order to calculate the slope of the enhancement spectra for $\text{CH}_4\text{-X}$, $X=\text{He}$ or Kr , by multiplying the experimental result for $\text{CH}_4\text{-Ar}$ (0.011) by the ratio $[\alpha_X^2 I(6)_{\text{CH}_4\text{-X}} / \alpha_{\text{Ar}}^2 I(6)_{\text{CH}_4\text{-Ar}}]$. For He the value of this ratio is 3.2×10^{-2} and, thus, the small value of the slope for $\text{CH}_4\text{-He}$ is consistent with the experimental observations.⁷ We can also generalize the theory to calculate the corresponding results for $\text{CH}_4\text{-X}_2$, where X_2 could be N_2 or H_2 , and for $\text{CH}_4\text{-CO}_2$ for which there are experimental data.^{7,11} These systems are of importance in the atmospheres of the outer planets and Venus.²⁷ This generalization requires three additional anisotropic quadrupole-induced dipole components of the form¹⁵

$$\begin{aligned} & \{ \langle 0J_1 | Q_{X_2} | 0J_1' \rangle \langle 0 | \gamma_{\text{CH}_4} | \nu_2 \rangle / R^4 \\ & \pm \langle 0J_1 | \gamma_{X_2} | 0J_1' \rangle \langle 0 | Q_{\text{CH}_4} | \nu_2 \rangle / R^4 \}^2. \end{aligned} \quad (15)$$

The matrix element $|\langle 0 | \gamma_{\text{CH}_4} | \nu_2 \rangle|$ is available from Raman measurements²⁸ and is negative.²⁹ The other parameters for N_2 , H_2 , and CO_2 are known. The results of these calculations, along with a discussion of the experimental details, will be presented elsewhere.¹¹ Suffice it to say that the overall agreement between theory and experiment leads us to the conclusion that the collision-induced quadrupolar mechanism is the dominant contribution to the enhancement spectra.

ACKNOWLEDGMENTS

Three of the authors (R.H.T., A.B., and Q.M.) would like to acknowledge support from NASA through Grant No. NAG5-8269, and J.L. thanks the Fonds National de la Recherche Scientifique de Belgique for financial support.

- ¹L. R. Brown, J. S. Margolis, J.-P. Champion, J. C. Hilico, J. M. Jouvard, M. Loete, C. Chackerian, Jr., G. Tarrago, and D. C. Benner, *J. Quant. Spectrosc. Radiat. Transf.* **48**, 617 (1992), and references therein.
- ²G. Birnbaum, *J. Chem. Phys.* **62**, 59 (1975); G. Birnbaum and E. R. Cohen, *ibid.* **62**, 3807 (1975).
- ³G. Birnbaum, A. Borysow, and A. Buechele, *J. Chem. Phys.* **99**, 3234 (1993).
- ⁴D. Pieroni, N. Van-Thanh, C. Brodbeck *et al.*, *J. Chem. Phys.* **110**, 7717 (1999).
- ⁵D. Pieroni, N. Van-Thanh, C. Brodbeck *et al.*, *J. Chem. Phys.* **111**, 6850 (1999).
- ⁶D. Pieroni, J.-M. Hartmann, F. Chaussard, X. Michaut, T. Gabbard, R. Santi-Loup, H. Berger, and J.-P. Champion, *J. Chem. Phys.* **112**, 1335 (2000).
- ⁷D. Pieroni, N. Van-Thanh, C. Brodbeck *et al.*, *J. Chem. Phys.* **113**, 5776 (2000).
- ⁸A. Levy, N. Lacombe, and C. Chackerian, Jr., in *Spectroscopy of the Earth's Atmosphere and Interstellar Medium*, edited by K. N. Rao and A. Weber (Academic, Boston, 1992).
- ⁹L. Frommhold, *Collision-Induced Absorption in Gases* (Cambridge U.P., Cambridge, 1993).
- ¹⁰V. A. Kondaurov, M. V. Kudryashova, S. M. Melokova, N. N. Filippov, and D. N. Shchepkin, *Opt. Spectrosc.* **81**, 373 (1996).
- ¹¹J.-M. Hartmann, R.H. Tipping, A. Brown, Q. Ma, and J. Lievin (to be published).
- ¹²L. S. Rothman, C. P. Rinsland, A. Goldman *et al.*, *J. Quant. Spectrosc. Radiat. Transf.* **60**, 665 (1998).
- ¹³J. Poll and J. L. Hunt, *Can. J. Phys.* **54**, 461 (1976).
- ¹⁴P. Dore, M. Moraldi, J. D. Poll, and G. Birnbaum, *Mol. Phys.* **66**, 355 (1989); G. Birnbaum, A. Borysow, and A. Buechele, *J. Chem. Phys.* **99**, 3234 (1993).
- ¹⁵R. H. Tipping and J. D. Poll, in *Molecular Spectroscopy: Modern Research*, Vol. III, edited by K. N. Rao (Academic, New York, 1985).
- ¹⁶G. Herzberg, *Molecular Spectra and Molecular Structure. II. Infrared and Raman Spectra of Polyatomic Molecules* (Van Nostrand Reinhold, New York, 1945).
- ¹⁷M. J. O'Loughlin, B. P. Reid, and R. K. Sparks, *J. Chem. Phys.* **83**, 5647 (1985).
- ¹⁸A. D. Buckingham, *Q. Rev., Chem. Soc.* **13**, 183 (1959).
- ¹⁹M. Herman, J. Lievin, J. Vander Auwera, and A. Campargue, *Adv. Chem. Phys.* **108**, 1 (1999).
- ²⁰MOLPRO (version 2000.1) is a package of *ab initio* programs written by H.-J. Werner and P. J. Knowles, with contributions from R. D. Amos, A. Bernhardsson, A. Berning *et al.*
- ²¹H.-J. Werner and P. J. Knowles, *J. Chem. Phys.* **89**, 5803 (1988); P. J. Knowles and H.-J. Werner, *Chem. Phys. Lett.* **145**, 514 (1988).
- ²²R. A. Kendall, T. H. Dunning, and R. J. Harrison, *J. Chem. Phys.* **96**, 6796 (1992).
- ²³H.-J. Werner and P. J. Knowles, *J. Chem. Phys.* **82**, 5053 (1985); P. J. Knowles and H.-J. Werner, *Chem. Phys. Lett.* **115**, 259 (1985).
- ²⁴J. Sun and K. Ruedenberg, *J. Chem. Phys.* **99**, 5257 (1993).
- ²⁵D. L. Gray and A. G. Robiette, *Mol. Phys.* **37**, 1901 (1979).
- ²⁶D. E. Stogryn and A. P. Stogryn, *Mol. Phys.* **11**, 371 (1966).
- ²⁷R. H. Tipping, in *Phenomena Induced by Intermolecular Interactions*, edited by G. Birnbaum (Plenum, New York, 1985).
- ²⁸T. Yoshino and H. J. Bernstein, *J. Mol. Spectrosc.* **2**, 241 (1958).
- ²⁹D. Bermejo, R. Escribano, and J. M. Orza, *J. Mol. Spectrosc.* **65**, 345 (1977).